Application of SQMFF Vibrational Calculations to Transition States: DFT and ab Initio Study of the Kinetics of Methyl Azide and Ethyl Azide Thermolysis

Juan F. Arenas,* Juan C. Otero, Adelaida Sánchez-Gálvez, and Juan Soto

Department of Physical Chemistry, Faculty of Sciences, University of Málaga, E-29071-Málaga, Spain

Pedro Viruela

Departament of Physical Chemistry, Universitat de València, Dr. Moliner 50, Burjassot, E-46100 València, Spain

Received: July 29, 1997; In Final Form: November 12, 1997

DFT including nonlocal corrections and ab initio calculations at MP2 and MP4 levels of theory have been performed in order to provide information concerning the mechanism of the rate limiting step of the thermal decomposition of methyl azide and ethyl azide. The chemically interesting points of the ground-state potential energy surface have been fully optimized, and a detailed normal-mode analysis for the reagents and the transition states is presented. The well-established scaled quantum mechanical force field method has been used to obtain reliable vibrational frequencies for these molecular structures. The force fields of transition states have been modified by using the scale factors computed for the force fields of the azides in their ground state. Finally, the activation energies and the Arrhenius preexponential factors for the rate constant have been computed according to transition state theory. The best values for the activation energies are provided by B3-LYP/6-311+G**. For the preexponential factor, the agreement with experiment seems to be independent of the level of theory used.

1. Introduction

The chemistry of organic azides has been widely developed in the last years. They constitute a versatile class of compounds used as important reagents in heterocycle syntheses[1] and in several biological methods.[2] For purpose of energy storage, these molecules are substantially higher in energy than their decomposition products, but with activation barriers sufficient for safe handling. Such characteristics have motivated their study as energetic additives for advanced solid propellants,[3−5] which is considered to be one of the practical ways to improve their technical performances. Energetic azides make a significant energy contribution to propellants and can also minimize the amount of flame and smoke in gases generated during the propulsion phase of solid propellants. In the past two decades, a large number of organic azides that find application in propellants have been synthesized and examined.[3−9] However, fundamental questions regarding the mechanism of the thermal decomposition of such molecules are not completely answered.

It is well-known from experimental results that the first step in the thermolysis of azides involves nitrogen elimination to yield the respective imine as the unique product.[10−14] The strong exothermic character of this step is responsible for the application of azides as propellants and for the chemical activation of the imine molecule, which consequently reacts to yield the final products: H_2, nitriles, hydrocarbons, etc.[13,14] The first-order overall kinetics of the thermolysis is controlled by the elimination of N_2 and two possible reaction pathways have been traditionally proposed for this process:[14] (a) A synchronous channel where both the elimination of nitrogen and the transposition of one substituent occur simultaneously as a concerted process, (b) An asynchronous channel, which occurs in two steps, in such a way that the azide first decomposes into N_2 and a singlet nitrene radical, that then transforms into an imine by transposition of one of the substituents. For years, it was generally accepted that the intermediate singlet nitrene existed, characterized by an extremely short lifetime, that rapidly suffered a Curtius rearrangement to yield the imine. When the C_s symmetry is considered in ab initio calculations,[15−17] the open-shell $^1A''$ of methylnitrene, which is a component of the Jahn−Teller splitting from ^1E state, is a local minimum with a high activation energy for rearrangement. Nevertheless, this process is irrelevant[16] in comparison with the rearrangement of the other Jahn−Teller component, singlet $^1A'$ methylnitrene, that is predicted to be a barrier-free process by several ab initio results.[15−19] Therefore, it has been proposed that singlet methylnitrene is not a genuine minimum on its potential energy surface, and this could explain why this species has never been detected in experiments neither of direct photolysis nor pyrolysis of methyl azide. Nevertheless, this radical has been experimentally observed by photodetachment spectroscopy of the CH_3N^- anion.[20] A singlet potential energy surface for the elimination of N_2 in methyl azide was obtained by Bock and Dammel[14] at MNDO level, and their results show that both the synchronous and the asynchronous channels compete since the activation energies at those level of theory are similar. However, these authors justify a preference for the synchronous path because the temperature of pyrolysis presents a substituent dependence. Recently, the geometry of the transition state involved in such a process has been localized at MP2/6-31G* level of theory by Nguyen *et al.*[21] and this channel has also been proposed for the direct photolysis of methyl azide,[22] although no definite experimental evidence exists up to date indicating which channel constitutes the reaction path.

S1089-5639(97)02500-0 CCC: $15.00
Published on Web 01/27/1998

In this paper we report a study of the possible pathways for their unimolecular decomposition for methyl azide and ethyl azide. For this purpose, MP2 and MP4 ab initio calculations and DFT methods including in all cases nonlocal corrections have been carried out. The preexponential factor for the rate constant has been computed according to transition state theory,[23] thus being necessary to compute the molecular partition function of the transition state $Z^{\ddagger}$ and that of the reagent Z. According to statistical mechanics, Z can be computed for the reagent using experimental data for the geometry, rotational constants, and vibrational frequencies. However, the respective data for the transition states are not yet experimentally accessible. To obtain reliable vibrational frequencies for them, we have used the well-established Pulay's method (SQMFF).[24] Quadratic force constants are scaled according to

$$F'_{ii} = \lambda_i F_{ii} \qquad \text{and} \qquad F'_{ij} = (\lambda_i \lambda_j)^{1/2} F_{ij}$$

where F_{ii} and F_{ij} are the quadratic quantum mechanically computed force constants, and F'_{ii} and F'_{ij} are the scaled ones, λ_i being the scale factors. The scale factors used for the force fields of the transition states have been obtained by transferring those computed for the azide molecule in its ground state.[25,26] The imaginary vibrational frequency is related to the negative eigenvalue of the Hessian matrix, and the corresponding normal mode must involve the bond that breaks (i.e., the vibrational degree of freedom that disappears to transform into a translational one).

2. Computational Methods

Semiempirical calculations were carried out by using the AM1 method as implemented in MOPAC 6.0,[27] and DFT and ab initio calculations were performed by using the program package GAUSSIAN 94.[28] All stationary points (i.e., equilibrium structures and transition states geometries) were fully optimized by gradient techniques at Hartree−Fock level using the 4-31G and 6-311G* basis sets. The effects of dynamic electron correlation were included using the second-order Møller−Plesset (MP) perturbation theory with full electron correlation, MP2-(Full), which includes the inner-shell electrons. To improve the energy predictions, particularly the barrier heights, single-point energy calculations MP4SDTQ with full electron correlation at the MP2 optimized geometries were also performed. The standard 6-311+G** basis set was used in all MP calculations. DFT computations were carried out in combination with 6-31G* and 6-311+G** basis sets. Up to date, Becke's three parameter (B3) gradient-corrected exchange functional[29] has been reported as the functional that predicts the best geometrical parameters and vibrational frequencies within the DFT framework.[24d] We have then used this hybrid method, where the nonlocal correlation has been provided by either Perdew and Wang's 1991 (PW91)[30] and the Lee−Yang−Parr (LYP)[31] gradient-corrected correlation functionals in order to compare the relative performance of both nonlocal exchange-correlation functionals in such a highly correlated system as the azide group. The harmonic frequencies were computed analytically for all optimized species with all mentioned levels of theory (a) to characterize each stationary point as a minimum or transition state, (b) to determine the zero point vibrational energy, and (c) to provide computational predictions of the force constant matrix that will be scaled using the SQMFF method for both the reagent structures and transition states.

3. Results and Discussion

3.1. Equilibrium Geometries. The equilibrium conformations of methyl azide and ethyl azide (Figure 1) have been the subject of many theoretical studies.[33−36] A detailed analysis of the dependence of the results on the basis set and on the inclusion of electronic correlation at MP2 level has been made by Costa Cabral et al.,[36] and therefore it will not be commented on here. To our knowledge no previous DFT results have been published for these molecules up to date. Geometric parameters for methyl azide and ethyl azide obtained at several levels of theory, including DFT, are collected in Table 1. Nonlocal DFT functionals previously described predict structural information very similar to the MP2 results, with differences with respect to the experimental data[37] ranging from 0.007 to 0.018 Å for bond lengths and up to 2.5° for the angles. More specifically, B3-LYP/6-311+G** and B3-PW91/6-31G* calculate the bond distances of the azide group which are in better agreement with the experimental values. All our theoretical calculations show that (a) the terminal $N_\beta N_\gamma$ distance is considerably shorter than the $N_\alpha N_\beta$ distance, (b) the azide group is not linear but slightly bent with an angle ∠NNN of 170−175°, in agreement with experimental MW data,[37] and (c) both in methyl azide and ethyl azide, H_1 is almost trans planar to the CNNN skeleton. In ethyl azide, such a disposition of H_1 (Figure 1) has been obtained from a full optimization of the geometrical variables and corresponds to the average conformation between the gauche and the anti conformers reported by Costa Cabral et al.[36]

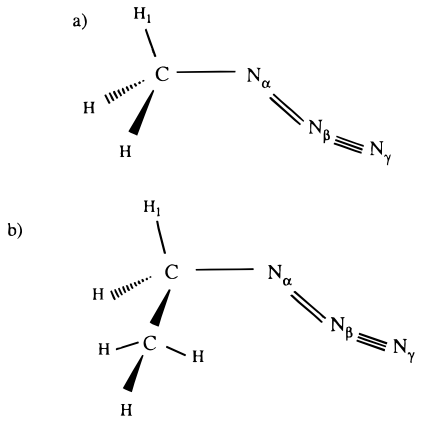

Figure 1. Equilibrium conformations of (a) methyl azide and (b) ethyl azide.

3.2. Potential Energy Surface. We have theoretically studied the ground-state decomposition of methyl azide and ethyl azide in the gas phase. Our first attempt to describe this process[26] was made at AM1 semiempirical level of theory by building a reduced potential energy surface (PES) where the $N_\alpha N_\beta$ bond length and H_1CN valence angle were chosen as independent variables. All the remaining defined internal coordinates were allowed to optimize. In the AM1 PES, asynchronous and synchronous reaction pathways shown in Scheme 1 are possible, in agreement with MNDO results obtained by Bock and Dammel.[14] Activation energies of both channels for methyl azide were very similar, amounting to 55.00 and 61.75 kcal/mol, respectively. For ethyl azide, E_{act}(async) = 55.41 kcal/mol and E_{act}(sync) = 59.16 kcal/mol. However, we have obtained different results when ab initio methods have been used. Our first calculations,[26] carried out with Hartree−Fock methodology, predicted that the mechanism of the thermal decomposition of simple alkyl azides follows the asynchronous path through TS2 transition state (see Scheme 1). At HF/4-31G and HF/6-311G* levels, the computed activation energies were very poor, and no TS1 transition state corresponding to the synchronous channel could be localized. Nevertheless, in the present work, which includes the electron correlation effects, no TS2 corresponding to the asynchronous path has been located

TABLE 1: Selected Geometrical Parameters[a] Computed for Methyl Azide (A) and Ethyl Azide (B) at Several Levels of Theory

	AM1		HF/ 4-31G		HF/ 6-311G*		MP2(Full)/ 6-311+G**		B3-LYP/ 6-31G*	B3-LYP/ 6-311+G**		B3-PW91/ 6-31G*	B3-PW91/ 6-311+G**	exptl
	A	B	A	B	A	B	A	B	A	A	B	A	A	A[b]
r(C−N)	1.440	1.450	1.482	1.490	1.465	1.473	1.474	1.481	1.474	1.474	1.484	1.466	1.466	1.483
$r(N_\alpha-N_\beta)$	1.254	1.253	1.243	1.242	1.224	1.223	1.238	1.237	1.235	1.229	1.229	1.230	1.224	1.231
$r(N_\beta-N_\gamma)$	1.136	1.136	1.114	1.115	1.096	1.096	1.155	1.156	1.143	1.136	1.136	1.142	1.134	1.137
$\angle H_1CN_\alpha$	103.6	102.1	105.7	104.2	106.6	105.0	106.4	104.7	106.4	106.6	104.7	106.5	106.7	106.8
∠CNN	121.9	121.9	116.0	115.9	113.4	113.7	114.8	114.8	115.7	116.1	116.2	116.0	116.3	113.85
∠NNN	168.7	169.0	172.2	172.5	175.4	175.5	172.6	172.9	172.9	173.1	173.3	172.9	173.1	173.1

[a] Distances in angstroms, angles in degrees. [b] From ref 37.

SCHEME 1: Mechanisms for the Unimolecular Decomposition of CH_3N_3 to $CH_2{=}NH + N_2$

a) Synchronous path

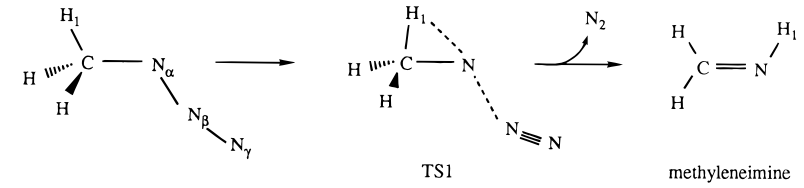

b) Asynchronous path

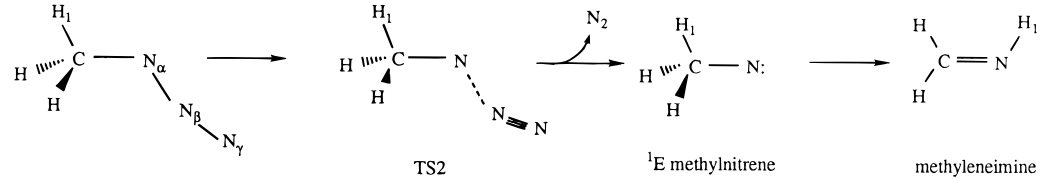

TABLE 2: Some Geometrical Parameters for Transition States of Methyl Azide (A) and Ethyl Azide (B) and Activation Energies for the Thermal Decomposition of Both Molecules Computed at *ab Initio* and DFT Levels of Theory

		$r(N_\alpha-N_\beta)$		∠(HCN)		E_{act}[a]	
theory level		A	B	A	B	A	B
HF/4-31G	TS2	1.608	1.606	101.8	99.94	9.89	9.75
HF/6-311G*	TS2	1.667	1.670	100.6	98.61	19.74	18.36
MP2(Full)/6-311+G**	TS1	1.900	1.869	88.70	85.96	49.03	47.92
						(43.30)	(45.78)
B3-LYP/6-31G*	TS1	2.075		86.79		44.19	
B3-LYP/6-311+G**	TS1	1.995	1.938	88.52	86.24	40.68	38.76
B3-PW91/6-31G*	TS1	2.068		83.59		49.52	
B3-PW91/6-311+G**	TS1	2.002		85.00		45.98	
exptl[b]						40.5	40.1

[a] Values (in kcal mol^{-1}) between parenthesis computed at MP4SDTQ(Full)/6-311+G**//MP2(Full)/6-311+G**. [b] From ref 10 for methyl azide and ref 11 for ethyl azide.

at all. These calculations, carried out with MP2(Full)/6-311+G** and with several nonlocal DFT functionals, predict that the breaking of the $N_\alpha-N_\beta$ bond and the Curtius rearrangement of the H_1 occur exclusively by a concerted process through the TS1 transition state (synchronous channel). We think that the lack of a TS1 on the HF potential energy surfaces and the poor values for the activation energies computed at those levels of theory are a consequence of the known insufficiencies of Hartree−Fock methods to correctly describe the behavior of molecular systems with long bond distances.

The calculated values of $r(N_\alpha-N_\beta)$ and $\angle H_1CN$ of the transition state involved in the concerted decomposition pathway of methyl azide and ethyl azide are given in Table 2. For HF/4-31G and HF/6-311G*, the transition state considered is TS2. The activation energies have been computed as the relative energies between the transition state and the minimum, always taking into account the thermal and the zero-point corrections, and they are also summarized in Table 2. At MP2(Full)/6-311+G** level, the $N_\alpha-N_\beta$ distance increases from 1.474 Å in methyl azide to 1.900 Å in TS1 and the H_1CN angle decreases from 106.4° to 88.70°. At this level of theory, the computed activation energy is overestimated in 8.53 kcal/mol. This result has been improved by carrying out single-point energy calculations with MP4SDTQ(Full)/6-311+G** using the geometries optimized at the MP2 level. The barrier height is then reduced to 43.30 kcal/mol, which is just 2.8 kcal/mol higher than the experimental value.[10]

By respect to DFT results, it is of interest to discuss the performance of the different functionals in foreseeing the transition state properties as barrier heights and structures, which has been done for methyl azide. Concerning DFT energy barriers, they are quite dependent on the type of functional and

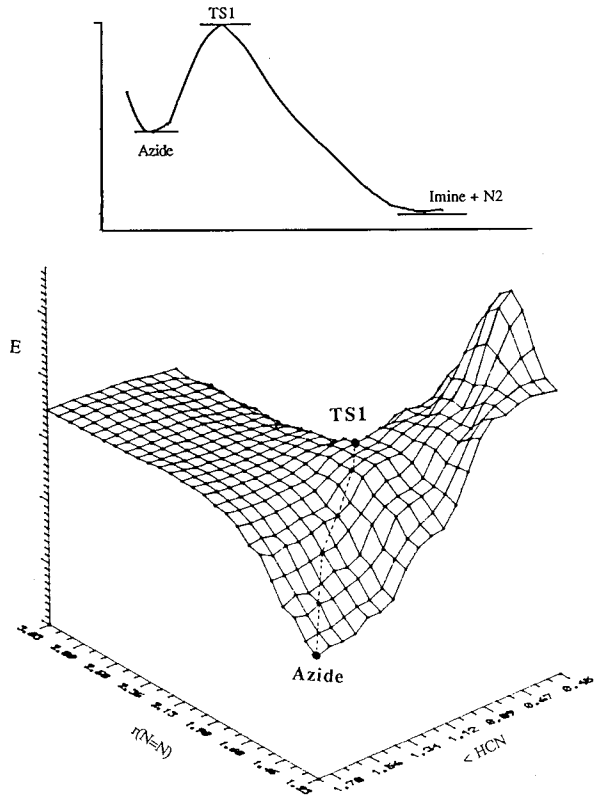

Figure 2. View of the B3-LYP/6-311+G** potential energy surface from the azide side and reaction profile for the thermal decomposition of methyl azide.

on the basis set which are used. B3LYP level predicts a better activation energy than B3PW91, and upon examining the quality of the two basis sets employed, we found that 6-311+G** always gives lower values for the activation energy than 6-31G*, thus giving a better agreement with experimental value.[13] With regard to the geometrical parameters computed for the transition state, B3LYP values are closer to the MP2 ones, and this agreement is better when the largest basis set 6-311+G** is used, given that the $r(N_\alpha-N_\beta)$ decreases and the $\angle H_1CN$ increases with respect to the 6-31G* values. The improvement of DFT results when higher basis sets are used has also been reported by Rauhut and Pulay,[24d] who found that, when polar systems as NH_2 or OH are studied, the 6-31G** basis set gives a better molecular description than 6-31G*. Therefore, we found that in the case of methyl azide, B3-LYP/6-311+G** gives the best DFT performance in foreseeing the transition state geometry and provides an excellent value of E_a, just 0.18 kcal/mol higher than the experimental one,[10] thus being the nonlocal functional that we will use for further calculations. As shown in Table 1 and Table 2, DFT data for ethyl azide were computed exclusively with that choice. To show the reaction surface for the thermal decomposition of methyl azide, Figure 2 gives a partial view of the B3LYP/6-311+G** potential energy surface as well as the energy profile that corresponds to the reaction path.

3.3. Scaled Vibrational Frequencies for Transition States. In this section a systematic method previously proposed[25,26] to obtain reliable vibrational frequencies for transition states is used. First, we have carried out normal coordinate analyses for the equilibrium structures and the TS1, which has been found as the relevant transition state involved in the rate limiting step of the thermolysis of alkyl azides. Vibrational spectra have been computed using all the levels of theory previously described. The fit to the experimental frequencies of methyl azide and ethyl azide in their ground state, reported by Nielsen et al.,[33b,38] has been performed by using the SQMFF method of Pulay.[24] Although DFT methods produce accurate molecular force fields and vibrational frequencies, they exhibit a systematic overestimation of the force constants that justifies the applicability of SQMFF methodology to DFT force constants, as clearly established by Rauhut and Pulay.[24d]

Force fields computed in symmetry coordinates have been transformed into internal coordinates because it allows for a better physical meaning of the force constants as well as for the scale factors transfer when the same internal coordinates are defined. Table 3 summarizes the diagonal force constants and the diagonal scale factors obtained in internal coordinates for methyl azide. The values of the scale factors can be considered as a criterion of the ability of a theoretical method to compute the force field. From this point of view, MP2 and B3-LYP are revealed to be the levels of theory that better reproduce the diagonal force constants of methyl azide.

An interesting feature of unimolecular reactions is that the transition state is a molecular species which still retains great similarity to the respective molecule in its ground state. Therefore, the same internal coordinates can be defined and it is also to be expected that quantum mechanical calculations of the force fields exhibit the same systematic deviations as in the ground state. Taking this into account, it seems to be quite sensible to propose that the scale factors computed for the azide can be transferred to the transition state in order to calculate its vibrational frequencies. Table 4 summarizes the scaled frequencies of TS1, as well as those of methyl azide obtained at the same levels of theory, and the experimental ones.[33b] According to the potential energy distribution (PED), the normal coordinate that corresponds to the imaginary frequency is described essentially by the stretching of the $N_\alpha=N_\beta$ bond that breaks in the first step of the elimination of N_2. There is also a considerable participation of CH_3 rocking in the imaginary frequency, because H_1 is moving from the C atom to the N atom. As a consequence of the weakening of the azide group in TS1, one observes also an important decrease in the frequencies of the bending normal mode δ(NNN), and the torsion $\tau(N_\alpha=N_\beta)$. On the other hand, the frequency of $\nu(N_\beta\equiv N_\gamma)$ increases significantly, because this bond becomes stronger in the process of N_2 elimination. MP2 and DFT methods present a very good agreement between them in the transition-state scaled frequencies. The only exception is the low frequency for $\nu(N_\beta\equiv N_\gamma)$ obtained with MP2 method when scale factors are transferred from the molecule in its ground state, 1992 cm^{-1}. This value is about 250 cm^{-1} lower than the computed one at B3-LYP level, and even lower than in the molecule in its ground state, 2106 cm^{-1}. We attribute this incorrect behavior of the MP2 method to two factors: (a) the force constant of $\nu(N_\beta\equiv N_\gamma)$ is calculated with a very similar value in TS1 and in the molecule in its ground state, thus not having the correct physical sense, and (b) the force field for the alkyl azide in its ground state is poorly calculated because the MP2 off-diagonal coupling force constant between the internal coordinates $\nu(N_\alpha=N_\beta)$ and ν $(N_\beta\equiv N_\gamma)$ in methyl azide has an anomalous value (-0.224 mdyn $Å^{-1}$) in comparison to AM1 (2.692), HF/4-31G (2.141), HF/6-311G* (2.384) and B3-LYP/6-311+G** (1.244). Such a value is responsible for the difficulties encountered in scaling the force field and the poorly scaled frequencies $\nu(N_\alpha=N_\beta)$ and $\nu(N_\beta\equiv N_\gamma)$ obtained for methyl azide at MP2 level (see Table 4). Nevertheless, this off-diagonal coupling force constant is well calculated for TS1, with a similar value (0.312) than the obtained with B3-LYP/6-311+G**

TABLE 3: Diagonal Scaled Force Constants and Diagonal Scale Factors for Methyl Azide in Internal Coordinates

	F_{ii}' [a]							scale factors λ_{ii}					
internal coordinates	exptl[b]	DZ SCF[c]	AM1	HF/ 4-31G	HF/ 6-311G*	MP2(Full)/ 6-311+G**	B3LYP/ 6-311+G**	DZ SCF[c]	AM1	HF/ 4-31G	HF/ 6-311G*	MP2(Full)/ 6-311+G**	B3LYP/ 6-311+G**
ν(C−H)			4.883	4.806	4.811	4.801	4.807		0.95	0.84	0.85	0.89	0.94
ν(N≡N)	*16.607*	*17.215*	*17.509*	*17.994*	*17.535*	*15.997*	*16.31*	*0.788*	*0.70*	*0.83*	*0.72*	*0.88*	*0.89*
δ(H−C−H)			0.516	0.457	0.459	0.472	0.476		1.11	0.775	0.80	0.93	0.96
δ(H−C−N)			0.620	0.602	0.599	0.617	0.614		0.98	0.80	0.79	0.94	0.97
ν(N=N)	*8.189*	*9.380*	*8.964*	*8.428*	*9.121*	*9.551*	*9.503*	*1.225*	*0.70*	*0.96*	*0.88*	*0.86*	*0.90*
ν(C−N)	4.890	4.407	4.995	4.913	4.301	4.661	4.544	0.982	0.63	1.00	0.79	0.95	0.99
δ(NNN)	0.758	0.624	0.619	0.642	0.586	0.606	0.594	0.788	1.24	1.15	0.85	0.92	1.01
δ(CNN)	0.628	0.952	0.952	0.913	0.920	0.920	0.909	0.696	0.75	0.75	0.77	1.11	0.99
τ(N=N)	0.598		0.026	0.012	0.004	0.011	0.009		1.53	1.09	0.80	1.33	1.03
τ(CH_3)		0.0067	0.023	0.020	0.018	0.018	0.018	0.621	0.54	0.91	0.72	0.56	0.73

[a] Stretching force constants in mdyn Å^{-1}. Bending force constants in mdyn Å rad^{-2}. [b] From ref 33b. [c] From ref 38.

TABLE 4: Scaled Vibrational Frequencies for TS1 at Several Levels of Theory and Comparison with the Experimental and Scaled Frequencies for Methyl Azide

	methyl azide			TS1[a]	
assignment	exptl[b]	MP2(Full/ 6-311+G**)	B3-LYP/ 6-311+G**	MP2(Full/ 6-311+G**)	B3-LYP/ 6-311+G**
ν_{as}'(CH_3)	3023	3030	3030	2885	2826
ν_{as}(CH_3)	2962	2958	2960	2770	2770
ν_{s}(CH_3)	2935	2938	2939	2873	2837
ν(N≡N)	*2106*	*2198*	*2112*	*2126*[c]	*2246*
δ_{as}'(CH_3)	1465	1469	1466	1517	1502
δ_{as}(CH_3)	1456	1453	1462	1246	1202
δ_{s}(CH_3)	1417	1421	1413	1311	1288
ν(N=N)	*1272*	*1255*	*1284*	*434i*	*282i*
r'(CH_3)	1132	1140	1129	1122	1116
r(CH_3)	1087	1087	1089	634	638
ν(C−N)	910	900	901	1220	1214
δ(NNN)	*666*	*672*	*661*	*142*	*144*
τ(N=N)	*560*	*565*	*558*	*97*	*112*
δ(CNN)	245	237	247	378	334
τ(CH_3)	100	107	103	324	341

[a] In cm^{-1}. [b] From ref 33b. [c] The corresponding force constant has not been scaled. When the ground-state scale factor is used, the computed vibrational frequency is 1992 cm^{-1}.

(0.371). Therefore, MP2 presents a different behavior in computing the force constants that involve the NNN stretching in TS1 and in the ground state. Consequently, the transference of the scale factors from the azide to the transition state has been done for all the internal coordinates excepting those that involve the NNN group, given that this level of theory does not obey the fundamental condition for a complete transfer of the scale factors from one molecular species to the other.

3.4. Preexponential Factors. According to transition state theory, the frequency factor for the rate constant is computed as follows:[25]

$$A = \frac{ekT}{h}\frac{Z^{\ddagger}}{Z}\exp\left[T\left(\frac{\partial \ln (Z^{\ddagger}/Z)}{\partial T}\right)_{p}\right]$$

where $Z^{\ddagger}$ is the molecular partition function of the transition state and Z is that of the azide in its ground state. Partition functions have been computed by using the optimized geometries, inertia moments and the scaled vibrational frequencies. The methyl group in methyl azide can be considered as a free internal rotor[39] and consequently the partition function must contain the respective factor. The preexponential factor A has been computed at $T = 500$ K as the reference temperature, given that the experimental data are reported at this particular temperature.[10,11]

Numerical values for A and E_{act} for both azides are collected in Table 5. The computed preexponential factors present a very good agreement with the experimental values for all the levels of theory, even when semiempirical and HF methods are used. This can be justified because, for both the computed geometries and the scaled frequencies, the numeric values obtained are not sufficiently different to alter the preexponential factor in a significant manner. To see whether the SQMFF method improves or not the preexponential factors, we have computed them for methyl azide as follows: (a) With calculated values of the frequencies (i.e., without any correction, the A-factors are 1.108×10^{14} for MP2(Full)/6-311+G** and 1.096×10^{14} for B3LYP/6-311+G**). (b) With corrected frequencies by using the scale factors 0.943 for MP2[40] and 0.963 for B3LYP,[24d] the A-factors are 1.174×10^{14} and 1.148×10^{14}, respectively. Objectively, SQM values shown in Table 5 agree better with experiment. Concerning the activation energy, the inclusion of electronic correlation effects yields an excellent agreement with experimental values.[10,11] For both methyl azide and ethyl azide, E_{act} computed with B3-LYP/6-311+G** is in better agreement with experiment than the corresponding MP2 and MP4 values.

TABLE 5: Experimental and Theoretical Values for Activation Energies and Preexponential Factors of the Thermal Decomposition of Methyl Azide and Ethyl Azide

	methyl azide		ethyl azide	
theory level	E_{act}[a]	A	E_{act}[a]	A
HF/4-31G[b]	9.89	0.98×10^{14}	9.75	0.61×10^{14}
HF/6-311G* [b]	19.74	1.86×10^{14}	18.36	1.05×10^{14}
MP2(Full)/6-311+G**	49.03 (43.30)	1.35×10^{14}	47.92 (45.78)	1.45×10^{14}
B3LYP/6-311+G**	40.68	1.22×10^{14}	38.76	1.10×10^{14}
exptl[c]	40.8	2.85×10^{14}	40.1	3.30×10^{14}

[a] Values between parenthesis (in kcal mol^{-1}) computed at MP4 SDTQ(Full)/6-311+G**//MP2(Full)/6-311+G** level of theory, and corrected with the thermal corrections, including ZPVE, obtained with MP2 (Full)/6-311+G**. [b] Value computed for the asynchronous channel, from ref 26. [c] From ref 10 for methyl azide and from ref 11 for ethyl azide.

4. Conclusions

The consideration of the electron correlation effects plays a significant role in the study of the thermal decomposition for simple alkyl azides, being essential for a correct theoretical discussion of the mechanism of the reaction and the identification of transition states. The inclusion of these effects has been made by using MP2 and MP4 ab initio calculations and density functional theory methods. At these levels of theory, the ground-state potential energy surface shows that the mechanism of rate-limiting step of this reaction follows a synchronous channel, where the breaking of the $N_{\alpha}-N_{\beta}$ and the Curtius

transposition of one of the substituents occur in a concerted way. No singlet nitrene is involved in this theoretical mechanism. B3-LYP in combination with the basis set 6-311+G** has been found as the nonlocal functional that better describes the properties of the transition state. Considering the moderate computational effort for DFT methods, it can be suggested as the standard level of theory for generating highly accurate results in the study of the alkyl azides. The force field scaling method has allowed to obtain reliable vibrational frequencies both for ground and transition states. Nevertheless, we found that MP2 shows anomalous behavior when computing force constants involving NNN stretching, and therefore, the respective scale factors must not be transferred to the transition state. Finally, activation energies and preexponential factors show a very good agreement with the experimental ones.

References and Notes

(1) (a) Scriven, E. F. V.; Turnbull, K. *Chem. Rev. (Washington, D.C.)* **1988**, *88*, 298 and references therein. (b) Zaragoza, F.; Petersen, S. V. *Tetrahedron* **1996**, *52*, 10823. (c) Vantinh, D.; Stadlbauer, W. *J. Heterocycl. Chem.* **1996**, *33*, 1025.

(2) (a) Schuster, G. B.; Platz, M. S. *Adv. Photochem.* **1992**, *17*, 69. (b) Mijer, E. W.; Nijhuis, S.; Van Vroohoven, F. C. B. M. *J. Am. Chem. Soc.* **1988**, *110*, 7209. (c) Matsumura, Y; Shiozawa, T; Matsushita, H.; Terao, Y. *Biol. Pharm. Bull.* **1995**, *18*, 1805. (d) Hicke, H. G.; Bohme, P.; Becker, M.; Schulze, H.; Ulbricht, M. *J. Appl. Polymer Sci.* **1996**, *60*, 1147.

(3) Liu, Y.-L.; Hsiue, G.-H.; Chiu, Y.-S. *J. Appl. Polymer Sci.* **1995**, *58*, 579.

(4) Kubota, N. *J. Propulsion Power* **1995**, *11*, 677.

(5) Sakata, J.; Wight, C. A. *J. Phys. Chem.* **1995**, *99*, 6584.

(6) Farber, M.; Harris, S. P.; Srisvastava, R. D. *Combust. Flame* **1984**, *55*, 203.

(7) Arenas, J. F.; Otero, J. C.; Soto, J. *J. Mol. Struct.* **1993**, *294*, 45.

(8) (a) Flanagan, J. E.; Wilson, E. R. U.S. Patent 4,427,466 **1984**. (b) Flanagan, J. E. U.S. Patent 4,797,168 **1989**.

(9) Schöyer H. F. R. et al. *J. Propul. Power* **1995**, *11*, 856.

(10) O′ Dell, M. S.; Darwent, B. DeB. *Can. J. Chem.* **1970**, *48*, 1140.

(11) Geiseler, V. G.; König, W. *Z. Phys. Chem. (Leipzig)* **1964**, *227*, 81.

(12) Pritzkow, W.; Timm, D. *J. Prakt. Chem.* **1986**, *32*, 178 (Russian).

(13) Bock, H.; Dammel, R. *Angew. Chem., Int. Ed. Engl.* **1987**, *26*, 506.

(14) Bock, H.; Dammel, R. *J. Am. Chem. Soc.* **1988**, *110*, 5261.

(15) Nguyen, M. T. *Chem. Phys. Lett.* **1985**, *117*, 290.

(16) Richards, C.; Meredith, C.; Khim, S.-J.; Quelch, G. E.; Schaefer, H. F. *J. Chem. Phys.* **1994**, *100*, 481.

(17) Sumathi, R. *J. Mol. Struct. (THEOCHEM.)* **1996**, *364*, 97.

(18) Demuynck, J.; Fox, D. J.; Yamaguchi, Y.; Schaefer, H. F. *J. Am. Chem. Soc.* **1980**, *102*, 6204.

(19) Pople, J. A.; Raghavachari, K.; Frisch, M. J.; Binkley, J. S.; Schleyer, P. v. R. *J. Am. Chem. Soc.* **1983**, *105*, 6389.

(20) Travers, M. J.; Cowles, D. C.; Clifford, E. P.; Ellison, G. B.; Engelking, P. C., quoted in ref 16.

(21) Nguyen, M. T.; Sengupta, D.; Ha, T.-K. *J. Phys. Chem.* **1996**, *100*, 6499.

(22) (a) Shang, H.; Yu, C.; Ying, L.; Zhao, X. *Chem. Phys. Lett.* **1995**, *236*, 318. (b) Ying, L. M.; Xia, Y.; Shang, H. R.; Tang, Y. Q. *J. Chem. Phys.* **1996**, *105*, 5798.

(23) (a) Eyring, H. *J. Chem. Phys.* **1935**, *3*, 107. (b) Wynne-Jones, W. F. K., Eyring, H. *J. Chem. Phys.* **1935**, *3*, 492, (c) Evans, M. G.; Polanyi, M. *Trans. Faraday Soc.* **1935**, *31*, 975.

(24) (a) Pulay, P.; Fogarasi, G.; Pang, F.; Boggs, J. E. *J. Am. Chem. Soc.* **1979**, *101*, 2550. (b) Pulay, P.; Fogarasi, G.; Boggs, J. E. *J. Chem. Phys.* **1981**, *74*, 3999. (c) Pulay, P.; Fogarasi, G.; Pongor, G.; Boggs, J. E.; Vargha, A. *J. Am. Chem. Soc.* **1983**, *105*, 7037. (d) Rauhut, G.; Pulay, P. *J. Phys. Chem.* **1995**, *99*, 3093 and references therein.

(25) Arenas, J. F.; Marcos, J. I.; Otero, J. C.; Sánchez-Gálvez, A.; Soto, J. *J. Chem. Soc., Faraday Trans.* **1996**, *92*, 363.

(26) Arenas, J. F.; Otero, J. C.; Sánchez-Gálvez, A.; Soto, J. *J. Mol. Struct. (THEOCHEM)* **1997**, *410*−*411*, 451.

(27) Stewart, J. P. MOPAC, Version 6.0, *QCPE* **1990**, *455*.

(28) GAUSSIAN 94, Revision D.3, Frisch, M. J.; Trucks, G. W.; Schlegel, H. B.; Gill, P. M. W.; Johnson, B. G.; Robb, M. A.; Cheesman, J. R.; Keith, T.; Petersson, G. A.; Montgomery, J. A.; Raghavachari, K.; Al-Laham, M. A.; Zakrzewski, V. G.; Ortiz, J. V.; Foresman, J. B.; Cioslowski, J.; Stefanov, B. B.; Nanayakkara, A.; Challacombe, M.; Peng, C. Y.; Ayala, P. Y.; Chen, W.; Wong, M. W.; Andres, J. L.; Replogle, E. S.; Gomperts, R.; Martin, R. L.; Fox, D. J.; Binkley, J. S.; Defrees, D. J.; Baker, J.; Stewart, J. P.; Head- Gordon, M.; González, C.; Pople, J. A. GAUSSIAN 94, Revsion 0.3; Gaussian, Inc.: Pittsburgh, PA, 1995.

(29) Becke, A. D. *J. Chem. Phys.* **1993**, *98*, 5648.

(30) Perdew, J. P.; Wang, Y. *Phys. Rev. B.* **1992**, *45*, 13244.

(31) Lee, C.; Yang, W.; Parr, R. G. *Phys. Rev. B.* **1988**, *37*, 785.

(32) Glidewell, C.; Holden, H. D. *J. Mol. Struct. (THEOCHEM)* **1982**, *89*, 325.

(33) (a) Sjøgren, C. E.; Nielsen, C. J. *J. Mol. Struct. (THEOCHEM)* **1986**, *142*, 285. (b) Klaeboe, P.; Nielsen, C. J.; Priebe, H.; Shei, S. H.; Sjøgren, C. E. *J. Mol. Struct. (THEOCHEM)* **1986**, *141*, 161. (c) Nielsen, C. J.; Sjøgren, C. E. *J. Mol. Struct. (THEOCHEM)* **1987**, *35*, 361.

(34) Costa, M. L. S. L.; Almoster Ferreira, M. A. *J. Mol. Struct. (THEOCHEM)* **1988**, *175*, 417.

(35) Palmer, M. H.; Guest, M. F. *Chem. Phys. Lett.* **1992**, *196*, 183.

(36) Costa Cabral, B. J.; Costa, M. L.; Almoster Ferreira, M. A. *J. Mol. Struct. (THEOCHEM)* **1993**, *281*, 185.

(37) Heineking, N.; Gerry, M. C. L. *Z. Naturforsch.* **1989**, *44a*, 669.

(38) Nielsen, C. J.; Kosa, K.; Priebe, H.; Sjøgren, C. E. *Spectrochim. Acta* **1988**, *44A*, 409.

(39) Salathiel, W. M.; Curl, R. F. *J. Chem. Phys.* **1966**, *44*, 1288.

(40) Apeloig, Y.; Albrecht, J. *J. Am. Chem. Soc.* **1995**, *117*, 9564.